

Density functionals with asymptotic-potential corrections are required for the simulation of spectroscopic properties of defects in materials.

Jeffrey R. Reimers,^{1,2} Rika Kobayashi,^{1,3} and Michael J. Ford^{1,2*}*

1 International Centre for Quantum and Molecular Structures and Department of Physics,
Shanghai University, Shanghai 200444, China.

2 University of Technology Sydney, School of Mathematical and Physical Sciences, Ultimo,
New South Wales 2007, Australia.

3 ANU Supercomputer Facility, Leonard Huxley Bldg. 56, Mills Rd, Canberra, ACT, 2601,
Australia.

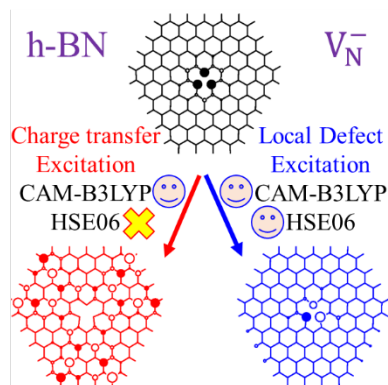
AUTHOR INFORMATION

Corresponding Author

* Jeffrey.Reimers@uts.edu.au, Mike.Ford@uts.edu.au

ABSTRACT The asymptotic potential error in modern density functionals is well known to adversely effect the energetics and structure of molecular excited states involving charge-transfer character. Here, we demonstrate that this effect also can be critical to the understanding of the spectroscopy of defects in materials, taking as an example the V_N^- defect in hexagonal boron nitride. The HSE06 density functional is used widely in advanced studies of materials defects but incorrectly represents the asymptotic potential. We show that it misrepresents the energetics of the excited states of the defect in a sample-size dependent manner, whereas the CAM-B3LYP density functional, which embodies long-range correction of the asymptotic potential, predicts results in accordance with those from MP2, CCSD, and CCSD(T) calculations. As a general rule, the entry-level for DFT calculations on the excited states of defects in materials should be considered to be use of functionals embodying long-range correction to the potential.

TOC GRAPHICS



KEYWORDS nanophotonics, single-photon emission, hexagonal boron nitride, charge-transfer transitions, range separated density functionals, density functional theory

Defects in hexagon boron nitride (h-BN) have been discovered that give rise to single-photon emission (SPE)¹⁻⁴ and optically detected magnetic resonance (ODMR),⁵⁻⁶ with many potential applications in nanophotonics.⁷⁻¹⁰ Historically, only defects displaying magnetic properties have had their chemical natures determined,^{5, 11-17} but recently came the first characterisation based only on observed spectral properties.¹⁸ This was made possible through extensive experimental characterisation of composition, combined with computational spectroscopic predictions. In general, the role of computation has been important in all defect assignments.¹³ For ground-state magnetic properties, many computational approaches such as density-functional theory (DFT), using generalized gradient approximation (GGA) or hybrid density functionals, deliver useful results and so progress has been rapid.

For spectroscopic properties, however, many difficult issues arise with both DFT and *ab initio* wavefunction approaches, with no method that is currently practical able to predict transition energies to within the desired accuracy of say ± 0.2 eV for all possible scenarios.¹⁹ Of tested methods, the most generally reliable approach is perhaps CAM-B3LYP,²⁰⁻²² which gives results within 0.5 eV of those from computationally demanding *ab initio* methods.¹⁹ This functional implements long-range corrections²³⁻²⁴ to the asymptotic potential by introducing range separation techniques²³ that dampen out²⁰ the LDA-based contribution to the exchange operator at long range, leaving this contribution dominated by the asymptotically correct Hartree-Fock-based contribution. Nevertheless, one of the most widely used density functionals is HSE06,²⁵⁻²⁶ a method that also embodies range separation,²³ but uses this feature instead to enhance computational efficiency by *removing* the Hartree-Fock contributions at long range.²⁶ Hence a key deficiency of the original PBE functional²⁷ upon which HSE06 is based is made prominent. For molecules, it has been demonstrated that density functionals that misrepresent

the asymptotic potential are subject to catastrophic failure should charge-transfer become a significant aspect of a spectroscopic transition of interest.²⁸⁻³¹ For defects in materials, predictions made using CAM-B3LYP and HSE06 can sometimes be very close to observed values,¹⁶ but often HSE06 predictions deviate significantly from those of CAM-B3LYP and *ab initio* approaches.^{19, 32}

To understand the fundamental nature of the problems associated with use of density functionals without long-range asymptotic-potential correction to model the properties of materials defects, we investigate transitions in the singlet and triplet manifolds of the V_N^- defect. This defect consists of a nitrogen-atom vacancy that is negatively charged; it has been considered for a long time³³⁻³⁴ as a possible contributor to observed h-BN spectroscopic properties, and of late also as a candidate for explaining some observed⁶ ODMR, but always not all calculated and observe properties appear to match. Of interest herein, the orbitals associated with the defect are predicted to lie close to the h-BN conduction band,^{16, 34} with the result that charge-transfer transitions with low energies will occur. This will amplify any effects associated with the failure of density functionals to treat charge transfer realistically.

As shown in Fig. 1, calculations are performed for the model compounds **1** – **4** of V_N^- that comprise rings of B and N atoms surrounding the nitrogen vacancy, as well as for the model 2D periodic layer **P64**. All molecular geometries are optimized using CAM-B3LYP/6-31G*, while the layer is optimized using HSE06; full details are provided in Supporting Information. Only vertical excitation energies are considered. The molecular calculations are performed using Gaussian-16,³⁵ while the periodic ones are performed using VASP³⁶⁻³⁷ (using “PREC=HIGH”, “PREFOCK=NORMAL”, PAW pseudopotentials,³⁸ at the Gamma-point of the Brillion zone of a $(6\times 4\sqrt{3})R30^\circ$ unit cell with lattice vectors depicting an intrinsic h-BN BN bond length of 1.452

Å). Model compounds for defects show very rapid convergence of calculated electronic properties with respect to increasing sample size pertaining to transitions localised mostly within the defect orbital space.^{17-18, 32} Of significance, such calculations have also been shown to converge to the same results as obtained using analogous calculations on 2D periodic defect models.³² Nevertheless, these generic results are not expected to apply to the transitions of V_N^- considered herein that involve the h-BN conduction band.

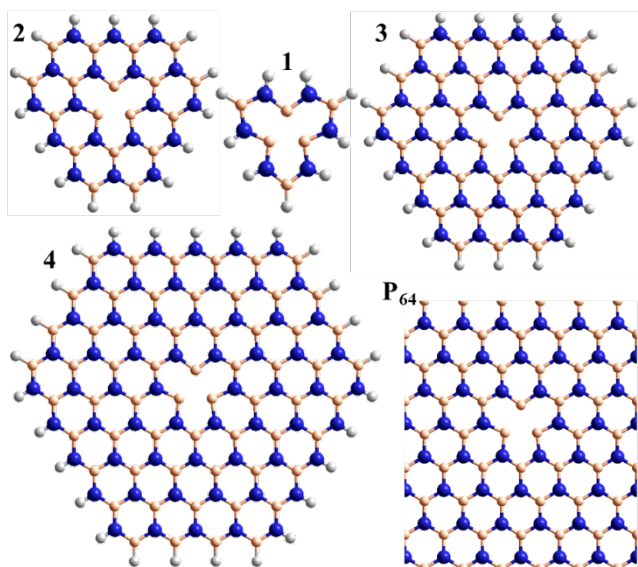


Fig. 1. Model compounds **1** – **4** and 2D layer **P₆₄** of the V_N^- defect in h-BN.

Table 1 provides excited-state energies obtained using time-dependent DFT (TD-DFT)³⁹ for the model compounds. TD-DFT is particularly well-suited to the study of defects as it only requires that its reference state be of mostly closed-shell nature, whereas most defect states are open shell,¹⁹ as indeed is the case for V_N^- . These energies are shown diagrammatically in Fig. 2(a)-(b). Model **1** only supports excitations within the defect core, with larger models adding in additional excitations that involve charge transfer to the h-BN conduction band. TD-CAM-B3LYP predicts that most transitions decrease in energy as the model size increases, with convergence quickly established. However, TD-HSE06 predicts that most states decrease

dramatically in energy as ring-size increases. The exceptions to this are the energies of $(1)^1E'$ and $(1)^3E'$, which quickly converge. The nature of the two key orbitals involved in excitations from the ground state to these states are shown in Fig. 2(d) and are both localized within the defect core. All other transitions, however, involve excitation to conduction-band orbitals, like the orbital shown in Fig. 2(d) that becomes occupied in the $(1)^1A'_2$ and $(1)^3A'_2$ states.

Table 1. Calculated vertical excitation energies, in eV, from the $(1)^1A'_1$ ground state of the model compounds **1** – **4** of the V_N^- defect in h-BN, obtained using time-dependent methods.

State	EOM-CCSD	TD-CAM-B3LYP				TD-HSE06			
	1	1	2	3	4	1	2	3	4
$(1)^1E''$	3.65	3.36	3.11	3.02	2.97	3.26	3.10	3.02	2.99
$(1)^1E'$	4.82	4.53*	3.79	3.64	3.63	4.25	2.78	2.21	1.85
$(2)^1E'$			4.09	3.85	3.74		3.42	2.69	2.26
$(1)^1A'_2$			3.54	3.77	3.62		2.52	2.59	1.81
$(2)^1A'_1$	5.47	5.20	4.67	3.61	3.84	4.77	3.85	2.10	2.20
$(1)^3E''$	3.09	2.77	2.33	2.21	2.18	2.66	2.27	2.16	2.13
$(1)^3E'$	3.65	3.19	2.73	2.62	2.58	2.99	2.47	2.18	1.85
$(2)^3E'$		5.28	3.75	3.61	3.59	4.87	2.78	2.39	2.22
$(1)^3A'_2$			3.46	3.71	3.61		2.43	2.54	1.80
$(1)^3A'_1$	4.86	4.43	4.32	3.60	3.82	3.97	3.51	2.08	2.19

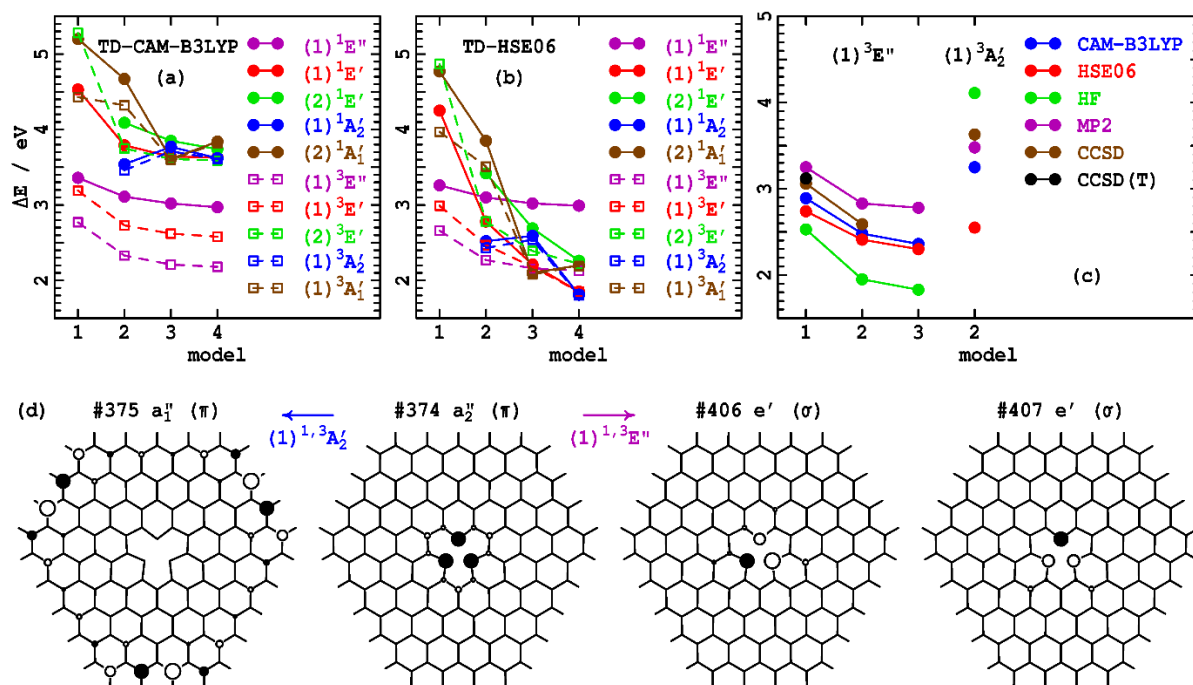


Fig. 2. Comparison of low-energy vertically excited singlet and triplet state vertical excitation energies (Tables 1 and 2) for varying ring-size models (Fig. 1) of the V_N^- defect of h-BN: (a)- by TD-CAM-B3LYP, (b)- by TD-HSE06, (c)- from DFT calculated state-energy differences. (d) shows the key orbitals of **4** involved in a localized defect transition and in a charge-transfer transition (CAM-B3LYP orbitals are shown, HSE06 ones are very similar).

The $(1)^1A_2''$ and $(1)^3A_2''$ states are highlighted as, for them, an occupied orbital is localized on the model boundary and hence could be considered as an artefact induced by using molecular cluster models. Indeed, for **2**, all charge transfer bands are by necessity located on the boundary. Models like **3** and **4** support centrally located charge-transfer states, and, for **4**, 17 charge-transfer transitions are predicted by TD-HSE06 at under 3 eV in energy, many of which

involve more central destination orbitals. The basic effect depicted is therefore a robust prediction of the calculations, though its quantitative nature is clearly model-size dependent.

Figure 2(d) lists the orbital numbers of the illustrated orbitals, with #374 being the HOMO orbital and #375 the LUMO. The CAM-B3LYP ordering is indicated and identifies $(1)^1A_2''$ and $(1)^3A_2''$ as resulting from the HOMO to LUMO transition; analogous HSE06 results are similar. Surprisingly, the low-energy states $(1)^1E'$ and $(1)^3E'$ arise from excitations deep into the unoccupied orbital space to orbitals #406 and #407. These are essentially defect orbitals, but their presence within the h-BN conduction band induces some mixing. As is often found for defects,¹⁹ orbital energy differences provide poor indications of state energy differences, particularly when charge transfer is involved.

Table 1 shows transition energies for **1** evaluated using equation of motion coupled cluster (EOM-CCSD) theory,⁴⁰ another time-dependent approach considered to provide useful descriptions of the singlet and triplet manifolds of V_N^- . It does not suffer from anomalies concerning its description of long-range electrostatic or charge-transfer effects, and its predictions are similar to those of CAM-B3LYP, but sometimes different to those of HSE06.

As an alternative to TD-DFT, we now consider transition energies evaluated by calculating individual DFT energies for both the initial and final states. This approach can only be applied to a limited selection of states, and is significantly hampered for V_N^- as DFT and many *ab initio* approaches fail owing to excited-state open-shell character. Qualitatively sensible results are obtained for the $(1)^3E'$ and $(1)^3A_2''$ states that are of particular interest, however, and results for **1** – **3** are listed in Table 2 and illustrated in Fig. 2(c). Used are the CAM-B3LYP and HSE06 density functionals, as well as the *ab initio* approaches: Hartree-Fock theory (HF),⁴¹ second-order Møller-Plesset (MP2) theory,⁴² coupled-cluster singles and doubles (CCSD)

theory,⁴³⁻⁴⁵ and this perturbatively corrected for triples excitations, CCSD(T).⁴⁶ For the local excitation $(1)^3E'$, the *ab initio* methods appear to converge quickly as the treatment of electron correlation is systematically enhanced, giving results close to those of CAM-B3LYP, with HSE06 deviating slightly further. For the charge-transfer excitation $(1)^3A_2''$, CAM-B3LYP deviates from CCSD by 0.4 eV, a large deviation but one consistent with other worst-case predictions obtained using CAM-B3LYP.¹⁹ On the other hand, HSE06 underestimates this energy by 0.9 eV.

Table 2. Calculated vertical excitation energies, in eV, from the $(1)^1A_1'$ ground state of the model compounds **1** – **4**, in D_{3h} symmetry, and the periodic layer **P₆₄**, in C_{2v} symmetry as necessitated by the boundary conditions, of the V_N^- defect in h-BN, obtained from state energy differences.

Method	$(1)^3E''$			$(1)^3A_2'$	$(1)^3B_1$
	1	2	3	2	P₆₄
CAM-B3LYP	2.89	2.48	2.48	3.25	
HSE06	2.74	2.41	2.41	2.55	1.57
HF	2.53	1.95	1.82	4.11	
MP2	3.25	2.83	2.72	3.48	
CCSD	3.06	2.59		3.63	
CCSD(T)	3.12				

Transition energies can also be obtained for periodic-layer models such as **P₆₄** from energy differences, but it is difficult to get results for all but the lowest-energy state of each

symmetry, and then only reasonable results can be expected if the two states of interest have minimal open-shell character. The energy gap between the highest-occupied defect orbital and the conduction band of V_N^- from 2D periodic-slab calculations has been reported at 1.8 eV,³⁴ and we find for \mathbf{P}_{64} a HSE06 value of 1.62 eV. The vertical excitation energy of the lowest triplet state is predicted to be 1.57 eV (Table 2). Owing to the use of boundary conditions in the periodic model, the defect, which should show both D_{3h} and its subgroup C_{2v} symmetry, cannot simultaneously display both 3-fold symmetry elements and the C_{2v} elements, with the utilized $(6\times 4\sqrt{3})R30^\circ$ lattice retaining only C_{2v} symmetry. The lowest excited triplet state is found to be $(1)^3B_1$, with a wavefunction that explores the boundary regions located far from the defect and hence is highly distorted from 3-fold symmetry. Orbital projection indicates that the lowest triplet state is comprised mostly of the HOMO to LUMO excitation from a defect b_1 (π) orbital to a conduction-band a_1 (σ) orbital. Even though the details differ significantly, owing to the boundary effect on charge-transfer transitions, the 2D periodic result parallels those from the model-cluster calculations in that charge transfer transitions are predicted by HSE06 to occur at unexpectedly low energies.

In conclusion, we see that, as is well known in molecular spectroscopy, DFT functionals without long-range corrections that restore the asymptotic potential to physically meaningful values seriously underestimate the energies of charge-transfer transitions. Such transitions abound in defect spectroscopy, but for most defects large separations between defect frontier orbitals and the valence and conduction bands of the surrounding material render the effect to be not critical. Nevertheless, poorly represented charge-transfer bands will influence defect-localized bands of typically greater interest. This effect is most likely responsible for the general poor performance of HSE06 found¹⁹ for defect-localized transitions. Methods such as CAM-

B3LYP that embody long-range correction and support for charge-transfer constitute the entry level for DFT calculations of defect spectroscopy. They are now appearing in codes with plane-wave basis sets that readily support calculations of 2D and 3D materials,³⁰ providing means to bound the likely errors that can arise during spectroscopic calculations on molecules and materials alike. Whilst the schemes for asymptotic potential correction applied herein were developed 15-20 years ago and are empirical in nature,^{20, 23} modern research is focusing on the developing density functionals by first principles that embody this effect.²⁴

ASSOCIATED CONTENT

Supporting Information. Geometries of all the structures used plus basic characterization is provided.

AUTHOR INFORMATION

Notes

The authors declare no competing financial interests.

ACKNOWLEDGMENT

This work was supported by resources provided by the National Computational Infrastructure (NCI) and Intersect, as well as Chinese NSF Grant #11674212. Computational facilities were also provided by the ICQMS Shanghai University High Performance Computer Facility.

Funding is also acknowledged from Shanghai High-End Foreign Expert grants to R.K. and M.J.F.

REFERENCES

1. Tran, T. T.; Bray, K.; Ford, M. J.; Toth, M.; Aharonovich, I., Quantum Emission from Hexagonal Boron Nitride Monolayers. *Nat. Nanotechnol.* **2016**, *11*, 37.
2. Tran, T. T.; Elbadawi, C.; Totonjian, D.; Lobo, C. J.; Grosso, G.; Moon, H.; Englund, D. R.; Ford, M. J.; Aharonovich, I.; Toth, M., Robust Multicolor Single Photon Emission from Point Defects in Hexagonal Boron Nitride. *ACS Nano* **2016**, *10*, 7331-7338.
3. Tran, T. T.; Zachreson, C.; Berhane, A. M.; Bray, K.; Sandstrom, R. G.; Li, L. H.; Taniguchi, T.; Watanabe, K.; Aharonovich, I.; Toth, M., Quantum Emission from Defects in Single-Crystalline Hexagonal Boron Nitride. *Phys. Rev. Appl.* **2016**, *5*, 034005.
4. Tawfik, S. A.; Sajid, A.; Fronzi, M.; Kianinia, M.; Tran, T. T.; Stampfl, C.; Aharonovich, I.; Toth, M.; Ford, M. J., First-Principles Investigation of Quantum Emission from Hbn Defects. *Nanoscale* **2017**, *9*, 13575-13582.
5. Gottscholl, A.; Kianinia, M.; Soltamov, V.; Bradac, C.; Kasper, C.; Krambrock, K.; Sperlich, A.; Toth, M.; Aharonovich, I.; Dyakonov, V., Room Temperature Initialisation and Readout of Intrinsic Spin Defects in a Van Der Waals Crystal. *Nat. Mater.* **2020**, *19*, 540-545.
6. Chejanovsky, N.; Mukherjee, A.; Kim, Y.; Denisenko, A.; Finkler, A.; Taniguchi, T.; Watanabe, K.; Dasari, D. B. R.; Smet, J. H.; Wrachtrup, J., Single Spin Resonance in a Van Der Waals Embedded Paramagnetic Defect. *arXiv:1906.05903* **2019**.
7. Awschalom, D. D.; Bassett, L. C.; Dzurak, A. S.; Hu, E. L.; Petta, J. R., Quantum Spintronics: Engineering and Manipulating Atom-Like Spins in Semiconductors. *Science* **2013**, *339*, 1174-1179.
8. Xia, F.; Wang, H.; Xiao, D.; Dubey, M.; Ramasubramaniam, A., Two-Dimensional Material Nanophotonics. *Nat. Photonics* **2014**, *8*, 899-907.
9. Aharonovich, I.; Englund, D.; Toth, M., Solid-State Single-Photon Emitters. *Nat. Photonics* **2016**, *10*, 631-641.
10. Lohrmann, A.; Johnson, B.; McCallum, J.; Castelletto, S., A Review on Single Photon Sources in Silicon Carbide. *Rep. Prog. Phys.* **2017**, *80*, 034502.
11. Feng, J.-W.; Zhao, J.-X., Theoretical Study of Oxidation of Monovacancies in Hexagonal Boron Nitride (H-Bn) Sheet by Oxygen Molecules. *J. Mol. Model.* **2014**, *20*, 2197.
12. Sajid, A.; Reimers, J. R.; Ford, M. J., Defect States in Hexagonal Boron Nitride: Assignments of Observed Properties and Prediction of Properties Relevant to Quantum Computation. *Phys. Rev. B* **2018**, *97*, 064101.
13. Sajid, A.; Ford, M. J.; Reimers, J. R., Single Photon Emitters in Hexagonal Boron Nitride: A Review of Progress. *Rep. Prog. Phys.* **2020**, *83*, 044501.
14. Abdi, M.; Chou, J.-P.; Gali, A.; Plenio, M., Color Centers in Hexagonal Boron Nitride Monolayers: A Group Theory and Ab Initio Analysis. *ACS Photonics* **2018**, *5*, 1967-1976.
15. Ivády, V.; Barcza, G.; Thiering, G.; Li, S.; Hamdi, H.; Legeza, Ö.; Chou, J.-P.; Gali, A., Ab Initio Theory of Negatively Charged Boron Vacancy Qubit in Hbn. *arXiv:1910.07767v1* **2019**.
16. Sajid, A.; Thygesen, K. S.; Reimers, J. R.; Ford, M. J., Assignment of Optically Detected Magnetic Resonance (Odmr) in Hexagonal Boron Nitride to the V_b^- and V_n^- Defects. *Commun. Phys.* **2020**, *in press* COMMSPHYS-19-0641B.
17. Reimers, J. R.; Shen, J.; Kianinia, M.; Bradac, C.; Aharonovich, I.; Ford, M. J.; Piecuch, P., The Photoluminescence and Photochemistry of the V_b^- Defect in Hexagonal Boron Nitride. *arXiv* **2020**.
18. Mendelson, N., et al., Identifying Carbon as the Source of Visible Single Photon Emission from Hexagonal Boron Nitride. *arXiv* **2020**, *2003.00949v3*.

19. Reimers, J. R.; Sajid, A.; Kobayashi, R.; Ford, M. J., Understanding and Calibrating Density-Functional-Theory Calculations Describing the Energy and Spectroscopy of Defect Sites in Hexagonal Boron Nitride. *J. Chem. Theory Comput.* **2018**, *14*, 1602-1613.
20. Yanai, T.; Tew, D. P.; Handy, N. C., A New Hybrid Exchange-Correlation Functional Using the Coulomb-Attenuating Method (Cam-B3lyp). *Chem. Phys. Lett.* **2004**, *393*, 51-57.
21. Kobayashi, R.; Amos, R. D., The Application of Cam-B3lyp to the Charge-Transfer Band Problem of the Zincbacteriochlorin–Bacteriochlorin Complex. *Chem. Phys. Lett.* **2006**, *420*, 106–109.
22. Cai, Z.-L.; Crossley, M. J.; Reimers, J. R.; Kobayashi, R.; Amos, R. D., Density-Functional Theory for Charge-Transfer: The Nature of the N-Bands of Porphyrins and Chlorophylls Revealed through Cam-B3lyp, Caspt2, and Sac-Ci Calculations. *J. Phys. Chem. B* **2006**, *110*, 15624-32.
23. Iikura, H.; Tsuneda, T.; Yanai, T.; Hirao, K., Long-Range Correction Scheme for Generalized-Gradient-Approximation Exchange Functionals. *J. Chem. Phys.* **2001**, *115*, 3540-44.
24. Carmona-Espíndola, J.; Gázquez, J. L.; Vela, A.; Trickey, S. B., Generalized Gradient Approximation Exchange Energy Functional with Correct Asymptotic Behavior of the Corresponding Potential. *J. Chem. Phys.* **2015**, *142*, 054105.
25. Krukau, A. V.; Vydrov, O. A.; Izmaylov, A. F.; Scuseria, G. E., Influence of the Exchange Screening Parameter on the Performance of Screened Hybrid Functionals. *J. Chem. Phys.* **2006**, *125*, 224106.
26. Heyd, J.; Scuseria, G. E.; Ernzerhof, M., Hybrid Functionals Based on a Screened Coulomb Potential. *J. Chem. Phys.* **2003**, *118*, 8207-8215.
27. Perdew, J. P.; Burke, K.; Ernzerhof, M., Generalized Gradient Approximation Made Simple. *Phys. Rev. Lett.* **1996**, *77*, 3865-3868.
28. Cai, Z.-L.; Sendt, K.; Reimers, J. R., Failure of Time-Dependent Density-Functional Theory for Large Extended Pi Systems. *J. Chem. Phys.* **2002**, *117*, 5543-9.
29. Peach, M. J. G.; Benfield, P.; Helgaker, T.; Tozer, D. J., Excitation Energies in Density Functional Theory: An Evaluation and a Diagnostic Test. *J. Chem. Phys.* **2008**, *128*, 044118.
30. Bircher, M. P.; Rothlisberger, U., Plane-Wave Implementation and Performance of Å-La-Carte Coulomb-Attenuated Exchange-Correlation Functionals for Predicting Optical Excitation Energies in Some Notorious Cases. *J. Chem. Theory Comput.* **2018**, *14*, 3184-3195.
31. Chai, J.-D.; Head-Gordon, M., Long-Range Corrected Hybrid Density Functionals with Damped Atom-Atom Dispersion Corrections. *Phys. Chem. Chem. Phys.* **2008**, *10*, 6615-6620.
32. Reimers, J. R.; Sajid, A.; Kobayashi, R.; Ford, M. J., Convergence of Defect Energetics Calculations. *arXiv* **2020**.
33. Katzir, A.; Suss, J.; Zunger, A.; Halperin, A., Point Defects in Hexagonal Boron Nitride. I. Epr, Thermoluminescence, and Thermally-Stimulated-Current Measurements. *Phys. Rev. B* **1975**, *11*, 2370.
34. Huang, B.; Lee, H., Defect and Impurity Properties of Hexagonal Boron Nitride: A First-Principles Calculation. *Phys. Rev. B* **2012**, *86*, 245406.
35. Frisch, M. J., et al., *Gaussian 16 Revision C.01*; Gaussian Inc.: Wallingford, CT, 2016.
36. Kresse, G.; Hafner, J., Ab Initio Molecular Dynamics for Liquid Metals. *Phys. Rev. B* **1993**, *47*, 558-561.
37. Kresse, G.; Furthmüller, J., Efficiency of Ab-Initio Total Energy Calculations for Metals and Semiconductors Using a Plane-Wave Basis Set. *Comput. Mat. Sci.* **1996**, *6*, 15-50.

38. Kresse, G.; Joubert, D., From Ultrasoft Pseudopotentials to the Projector Augmented-Wave Method. *Phys. Rev. B* **1999**, *59*, 1758.
39. Casida, M. E., Time-Dependent Density Functional Response Theory for Molecules. In *Recent Advances in Density Functional Methods, Part 1*, Chong, D. P., Ed. World Scientific: Singapore, 1995; pp 155-192.
40. Stanton, J. F.; Bartlett, R. J., The Equation of Motion Coupled-Cluster Method. A Systematic Biorthogonal Approach to Molecular Excitation Energies, Transition Probabilities, and Excited State Properties. *J. Chem. Phys.* **1993**, *98*, 7029-7039.
41. Fock, V., "Selfconsistent Field" Mit Austausch Für Natrium. *Zeitschrift für Physik* **1930**, *62*, 795-805.
42. Møller, C.; Plesset, M. S., *Phys. Rev. A* **1934**, *46*, 618.
43. Čížek, J., On the Correlation Problem in Atomic and Molecular Systems. Calculation of Wavefunction Components in Ursell-Type Expansion Using Quantum-Field Theoretical Methods. *J. Chem. Phys.* **1966**, *45*, 4256-4266.
44. Čížek, J., On the Use of the Cluster Expansion and the Technique of Diagrams in Calculations of Correlation Effects in Atoms and Molecules. *Adv. Chem. Phys.* **1969**, *14*, 35-89.
45. Paldus, J.; Íek, J.; Shavitt, I., Correlation Problems in Atomic and Molecular Systems. Iv. Extended Coupled-Pair Many-Electron Theory and Its Application to the Bh_3 Molecule. *Phys. Rev. A* **1972**, *5*, 50-67.
46. Raghavachari, K.; Trucks, G. W.; Pople, J. A.; Head-Gordon, M., A Fifth-Order Perturbation Comparison of Electron Correlation Theories. *Chem. Phys. Lett.* **1989**, *157*, 479-483.